Design Guidelines in Nonconventional Composite Laminate Optimization

Peeters, Daniel; Abdalla, Mostafa

DOI
10.2514/1.C034087

Publication date
2016

Document Version
Accepted author manuscript

Published in
Journal of Aircraft: devoted to aeronautical science and technology

Optimisation of ply drop locations in Variable Stiffness Composites

Daniël Peeters* and Mostafa Abdalla†

Delft University of Technology, 2629 HS Delft, The Netherlands

A method for optimising ply drop locations in composite laminates is developed using ideas from topology optimisation. The design is parametrised using a fibre angle and fictitious density distribution for each ply. The solution proceeds using a successive conservative convex approximations strategy. The structural responses are approximated separately in terms of the angle and fictitious density distributions of each ply. Explicit penalisation of intermediate densities is used to force the densities to either one, ply coverage, or zero, no coverage. Ply drop locations are identified as the boundary between regions having densities near one and those near zero. The ply drop optimisation is combined with fibre angle optimisation by alternating the optimisation between the corresponding set of variables. Optimised variable stiffness, variable thickness composite laminates are obtained. Initial results show that large improvements in buckling load of flat plates can be obtained by combining ply drop and fibre angle optimisation.

I. Introduction

Composite materials are attractive due to their high stiffness-to-weight and strength-to-weight ratio. It has been shown that by spatially varying the stiffness, even better performance can be obtained without adding extra weight. Varying the stiffness can be done in two ways: either by changing the fibre angles, by steering the fibres, or by changing the number of plies from one point to the next by dropping plies. To develop constant thickness, steered laminates, a three-step optimisation approach has been developed.[1,2] In the first step the optimal stiffness distribution in terms of lamination parameters is found, in the second step the optimal fibre angles at each node are obtained, and in the third step the optimal fibre paths are retrieved. A thickness variation has already been implemented in the first step of the optimisation, and showed that significant improvements could be obtained,[1] however, no information about fibre angle or number of plies is available at the first step, so the physical construction of the laminate remains to be found.

Thickness variation in a laminate is described using two variables: the ply drop location and the ply dropping order. The most popular approach is to use an evolutionary algorithm, typically a genetic algorithm, to optimise the number of layers per 'patch', while also optimising the ply dropping order and stacking sequence, limited to a discrete set of angles (e.g., 0°, ±45°, and 90°). This area of research is referred to as laminate blending[3–7] and assumes that potential ply drop locations (i.e., patch boundaries) are pre-specified by the user. A technique where the fibre angle is not restricted to a discrete set has also been developed, however, no manufacturing constraints, limiting the change in fibre angle from one element to the next, are posed.[8]

Other techniques where the ply drop locations are not pre-specified use continuous optimisation. Shape optimisation[9] is used to determine the shape and hence ply coverage and ply drop locations of the different layers. The optimisation is performed using a level-set approach with fibre angles limited to a discrete set. Another continuous method is the discrete material and thickness optimisation method, where the fibre angles belong to a discrete set and fictitious density variables are used to select the ply angles at any given location. This has been done for compliance and buckling optimisation.[10,11] For this method, also

*Ph.D. Student, Faculty of Aerospace Engineering, Aerospace Structures and Computational Mechanics, Kluyverweg 1; D.M.J.Peeters@tudelft.nl; Student member AIAA

†Associate Professor, Faculty of Aerospace Engineering, Aerospace Structures and Computational Mechanics, Kluyverweg 1; M.M.Abdalla@tudelft.nl

a thickness filter has been implemented to get to physically feasible designs.[12] Thickness optimisation for buckling load under uni- and bi-axial compression has also been performed. This work showed that large improvement in buckling load could be made without affecting the in-plane stiffness.[13]

A method to optimise ply drop location and fibre angle distribution, where ply angles are not restricted to a discrete set and ply drop locations are not pre-specified, is described in this paper. The method is based on the use of fictitious density distributions similar to classical topology optimisation. The remainder of this paper is organised as follows: first, the parametrisation in terms of the densities is discussed in section II, then the optimisation problems are stated in section III and the solution procedure is given in section IV. The post processing steps are briefly discussed in section V, followed by some results in section VI, and finally the conclusion in section VII.

II. Design Parametrisation

Structural responses can be written, for symmetric laminates, as a function of the material in-plane stiffness matrix $\boldsymbol{A}$ and out-of-plane stiffness matrix $\boldsymbol{D}$. It is assumed the laminate is symmetric, hence the membrane-bending coupling matrix $\boldsymbol{B} = \boldsymbol{0}$. The $\boldsymbol{A}$ and $\boldsymbol{D}$ matrix are defined as[14]

$$\begin{aligned} \boldsymbol{A} &= 2 \cdot \sum_{k=1}^{L} \bar{\boldsymbol{Q}}_k(\theta_k) \cdot \left(z_{k-1} - z_k\right) \\ \boldsymbol{D} &= 2 \cdot \frac{1}{3} \sum_{k=1}^{L} \bar{\boldsymbol{Q}}_k(\theta_k) \cdot \left(z_{k-1}^3 - z_k^3\right) \end{aligned} \tag{1}$$

The sum is extended over all plies starting from the top layer; L denotes the number of plies in the symmetric part, z_{k-1} denotes the distance from the reference plane to the top side of the k^{th} ply, and z_k to the bottom side of the k^{th} ply, as can be seen on the left in Figure 1. The thickness of the k^{th} ply is given by

$$t_k = z_{k-1} - z_k. \tag{2}$$

The total laminate thickness h is given by

$$h = 2 \cdot \sum_{k=1}^{L} t_k. \tag{3}$$

If the reference plane is chosen as the mid-plane of the laminate, then

$$z_0 = h/2. \tag{4}$$

Hence, the z-coordinates can be expressed as

$$z_k = \sum_{i=1}^{L} t_i - \sum_{i=1}^{k} t_i. \tag{5}$$

The purpose of the parametrisation is to include the ability to drop individual plies into the design process. To accomplish this, a fictitious density ρ_k is introduced for each layer. The fictitious density distribution represents the degree of presence of the material: a density near one indicating the ply *covers* a particular location and a density near zero indicating no coverage. The ply drop locations are thus where the density changes from near one to near zero.

Introducing the density per ply for the $\boldsymbol{A}$ matrix is done analogously to the previous work by the authors[15] by penalisation. First, the in-plane stiffness is written in the form

$$\boldsymbol{A} = 2 \cdot \sum_{k=1}^{L} \boldsymbol{A}_k, \boldsymbol{A}_k = t_k \bar{\boldsymbol{Q}}_k(\theta_k), \tag{6}$$

then penalisation per layer is introduced:

$$\boldsymbol{A} = 2 \cdot \sum_{k=1}^{L} \rho_k^p \cdot \boldsymbol{A}_k. \tag{7}$$

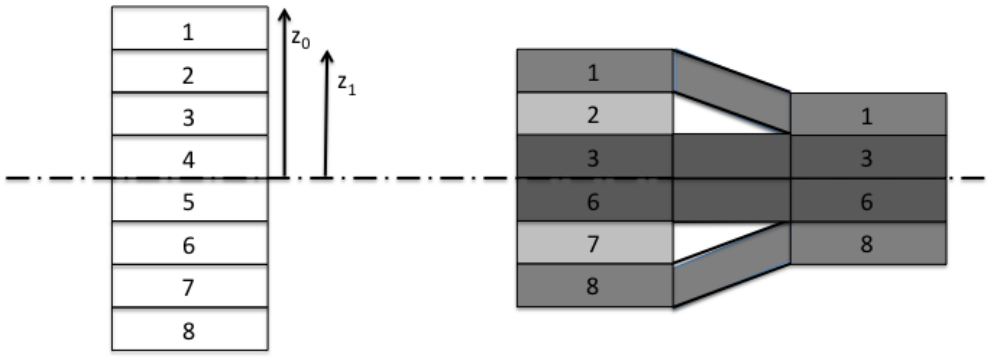

Figure 1. z-coordinates of the different plies and ply drop example

where p denotes the penalisation power. Since explicit penalisation will be used, p equals one and will be omitted in the remainder of the paper.

To reflect the reduced material presence on the weight of the laminate, individual layer thickness is modified to be a function of the corresponding density:

$$t_k = t_k^0 \cdot \rho_k, \tag{8}$$

where t_k^0 is the physical layer thickness of the k^{th} layer.

The dependence of the z-coordinates on the densities is found from equation (5):

$$z_k(\boldsymbol{\rho}) = \sum_{i=1}^{L} \rho_i \cdot t_i^0 - \sum_{i=1}^{k} \rho_i \cdot t_i^0. \tag{9}$$

The dependence of the bending stiffness $\boldsymbol{D}$ follows directly from equations (7) and (9):

$$\boldsymbol{D} = \frac{2}{3} \sum_{k+1}^{L} \rho_k \cdot \boldsymbol{A_k} \cdot \left(z_k(\boldsymbol{\rho})^2 + z_k(\boldsymbol{\rho}) \cdot z_{k-1}(\boldsymbol{\rho}) + z_{k-1}(\boldsymbol{\rho})^2 \right) \tag{10}$$

where $\boldsymbol{\rho}$ is a vector of the densities of all layers in the symmetric part.

The layers with zero density are dropped for the limiting case where each ρ equals either one or zero. An example is shown in Figure 1. To the left is depicted the full stack of layers representing the maximum number of plies. This can be thought of as a 'guide laminate', used in laminate blending algorithms,[16] from which actual laminates are derived by dropping some of the layers. To the right, a transition region around a ply drop is depicted. The local density vector changes from $\boldsymbol{\rho} = [1, 1, 1, 0, 0, 1, 1, 1]$ to $\boldsymbol{\rho} = [1, 0, 1, 0, 0, 1, 0, 1]$.

Since a gradient-based optimiser is used, the derivative of the $\boldsymbol{A}$ and $\boldsymbol{D}$ matrices with respect to densities are needed:

$$\begin{aligned} \frac{\partial \boldsymbol{A}}{\partial \rho_k} &= 2\boldsymbol{A_k} \\ \frac{\partial \boldsymbol{D}}{\partial \rho_k} &= \frac{2}{3}\boldsymbol{A}_k \cdot \left(z_k^2 + z_k \cdot z_{k-1} + z_{k-1}^2 \right) + \\ &\quad \frac{2}{3} \sum_{i=k}^{L} \rho_i \cdot \boldsymbol{A}_i \cdot t_i^0 \cdot \left(2 \cdot z_i + z_{i-1} \right) + \frac{2}{3} \sum_{i=k-1}^{L} \rho_i \cdot \boldsymbol{A}_i \cdot t_i^0 \cdot \left(z_i + 2 \cdot z_{i-1} \right) \end{aligned} \tag{11}$$

Using these equations the $\boldsymbol{A}$ and $\boldsymbol{D}$ matrices can be linearised in terms of ply densities. Having a balanced laminate is another property that is often required in composite design. This reduces the number of *design layers* further since every layer will have a balanced counterpart: the negative of the fibre angle, and the same density. Hence, if symmetry is also imposed, each design layer represents four layers in the physical laminate. The balanced layer can be anywhere in the stack, the location of the balanced layers is pre-defined by the user. In the remainder, L denotes the number of design layers.

In the proposed formulation, individual design layers may be dropped or maintained at any given location. In composite design, guidelines for ply dropping to maintain structural integrity exist. One of the most important requirements[16,17] is to maintain an adequate ply drop schedule. While many ply drop schedules would be compatible with the guidelines, choosing the optimum schedule for a particular design problem is a difficult combinatorial optimisation problem: the drop schedule has to be the same at each point, while the optimum at each point may be different. In this paper, we assume that a ply drop schedule that satisfies the guidelines has been pre-selected by the designer. The ply dropping schedule is specified by a vector $\boldsymbol{d}$ such that ply d_i is the i^{th} ply to be dropped. For example, the schedule $\boldsymbol{d} = [4, 2, 3, 1]$ means ply 4 is dropped first, then plies 2, 3 and finally 1, the outer ply. In this example no balancing constraint is posed. If a balancing constraint is imposed, the balanced layers drop at the same point; only one number per design layer appears in the dropping schedule $\boldsymbol{d}$. The possibilities to drop plies include inner and outer blending,[18,19] but are not limited to these. To enforce the ply drop schedule in the optimisation problem, the following $L-1$ constraints are adduced:

$$\rho_{\boldsymbol{d}_1} \leq \rho_{\boldsymbol{d}_2} \leq \cdots \leq \rho_{\boldsymbol{d}_L} \tag{12}$$

The structure to be optimised is modelled using finite elements. The design variable are defined at the nodes, and the properties are 'smeared' to the elements using

$$\boldsymbol{A_e}^{-1} = \frac{1}{3}\sum_{i=1}^{3} \boldsymbol{A_i}^{-1} \tag{13}$$

since triangular elements are used. The design variables are defined at the nodes of the finite element mesh for two reasons: the gradient constraint on fibre angles, see sec. III, requires C^0 continuity, and it is well known that forcing a continuous density distribution avoids checker board patterns in topology optimisation.[20] The vectors of design variables $\boldsymbol{\rho}$ and $\boldsymbol{\theta}$ are partitioned into sub-vectors denoting the properties at a given node:

$$\begin{aligned} \boldsymbol{\rho} &= (\boldsymbol{\rho}_1|\boldsymbol{\rho}_2|...|\boldsymbol{\rho}_N) \\ \boldsymbol{\theta} &= (\boldsymbol{\theta}_1|\boldsymbol{\theta}_2|...|\boldsymbol{\theta}_N) \end{aligned} \tag{14}$$

where N denotes the number of nodes. Each sub-vector is composed of the fibre angles θ_j or fictitious densities ρ_j at each layer, with j ranging from 1 to L. The feasible region $\mathcal{D}_i$ is defined as

$$\begin{aligned} \rho_\ell \leq \rho_j \leq 1, j = 1, \cdots, L \\ \frac{-\pi}{2} \leq \theta_j \leq \frac{\pi}{2}, j = 1, \cdots, L \end{aligned} \tag{15}$$

The lower bound on density ρ_ℓ is ideally zero, but is set to a small number, typically 10^{-3}, to avoid a singular stiffness matrix, following the standard practice in topology optimisation. If some layers are not allowed to be dropped, for example to enforce minimum gauge thickness or surface coverage, the density of these layers is fixed to one, and the lower bound of the other layers may be set to zero without a singular stiffness matrix appearing.

III. Optimisation

In structural optimisation, the minimisation of an objective response (e.g., weight or compliance) subject to performance constraints (e.g., on stresses or displacements) is studied. More generally, the worst case response, for example in the case of multiple load cases, is optimised. Additional constraints not related to structural responses may also be imposed to guarantee certain properties of the design such as manufacturability. The following general problem formulation is considered:

$$\begin{aligned} \min_{\boldsymbol{\rho},\boldsymbol{\theta}} \quad & \max(f_1, f_2, ..., f_n) \\ s.t. \quad & f_{n+1}, ..., f_m \leq 0 \\ & V \leq \eta \cdot V_0 \\ & \boldsymbol{\rho}, \boldsymbol{\theta} \in \mathcal{D}_i \end{aligned} \tag{16}$$

where V is the material volume, η is the maximum allowed volume fraction, and V_0 is the total domain volume. The functions f_i depend on the design variables; f_1 to f_n denote structural responses that are

optimised and f_{n+1} up to f_m denote structural responses that are constrained. This problem will be solved using successive approximations: one starts from a certain fibre angle and fictitious density distribution, constructs the approximations, optimises the approximations and updates the approximations based on the new distributions. This is repeated until convergence is reached, which is defined in this work as less than 10^{-3} change in objective function between consecutive finite element (FE) analyses, normalised with respect to the quasi-isotropic behaviour.

A known problem in topology optimisation is making the fictitious densities ρ converge to either one, indicating the presence of material, or zero, indicating a void, the black-and-white design. It was shown in previous work[15] that implicit and explicit penalisation have comparable performance in topology optimisation of composites. In this paper, only explicit penalisation is used. Explicit penalisation works by defining a measure of grey area as

$$g = \frac{\sum_{i=1}^{N} \alpha_i \cdot (\rho_i - \rho_\ell) \cdot (1 - \rho_i)}{V_0} \tag{17}$$

and forces a reduction in g until an acceptable black-and-white design is obtained. Acceptable means that the topology of each layer should be clear. This means the grey area g should be less than 10^{-2}: this implies all values for density are close to 0 or 1 and the topology is clear. The variable α_i is the volume associated with the i^{th} node.

Structural responses, such as buckling loads, stiffness, and strength, are calculated using a FE analysis. Since each FE analysis is computationally expensive, greater efficiency can be achieved by using structural approximations to reduce the required number of FE analyses.[21,22] The exact FE response f is first approximated in terms of the in- and out-of-plane stiffness matrices $\boldsymbol{A}$ and $\boldsymbol{D}$ and their reciprocals:[1]

$$f^{(1)} \approx \sum_{n=1}^{N} \boldsymbol{\phi}_m : \boldsymbol{A}^{-1} + \boldsymbol{\phi}_b : \boldsymbol{D}^{-1} + \boldsymbol{\psi}_m : \boldsymbol{A} + \boldsymbol{\psi}_b : \boldsymbol{D} + c \tag{18}$$

where the : operator represents the Frobenius inner product, $\boldsymbol{A} : \boldsymbol{B} = tr(\boldsymbol{A} \cdot \boldsymbol{B}^T)$; $\boldsymbol{\phi}$ and $\boldsymbol{\psi}$ are calculated from sensitivity analysis.[23,24] Subscripts m and b denote the membrane and bending parts respectively. This approximation is a generalisation of the linear-reciprocal approximations used in the convex linearisation method.[25] The approximations are convex functions in stiffness space provided that $\boldsymbol{\phi} \geq 0$, a condition that is always satisfied by construction. The free term c equals zero for many types of responses that enjoy homogeneity properties.

A. Ply drop optimisation

The approximation in (18) is convex in terms of the stiffness,[26] but not in terms of the density distribution, hence a second level approximation is required. Linear approximations in terms of densities are used for all responses. The gradient with respect to densities is calculated using the chain rule starting from (18) and using (11).

Following a similar strategy to the earlier work on combining topology and laminate optimisation,[15] the optimisation is performed in two steps: first the optimal structural response is found regardless of the amount of grey, and, second, the amount of grey is minimised, while allowing the structural performance to deteriorate slightly.[15]

In the first step of the optimisation, the density is assumed to be the same for all layers, hence $\boldsymbol{\rho}$ is a vector of length N containing the density at each node in the FE model. This effectively leads to a combined total thickness and fibre angle optimisation. The optimisation problem for densities can be written as

$$\begin{aligned} \min_{\boldsymbol{\rho}} \quad & \max(f_1, f_2, ..., f_n) \\ s.t. \quad & f_{n+1}, ..., f_m \leq 0 \\ & V \leq \eta \cdot V_0 \\ & \rho_\ell \leq \rho_i \leq 1 \qquad i = 1, ..., N \end{aligned} \tag{19}$$

After this first step, the structural responses are optimised but the density distribution will, most likely, contain a lot of grey area. In the second step, $\boldsymbol{\rho}$ is a matrix which denotes the density of each layer at each

node. The amount of grey area is minimised:

$$\begin{array}{lll} \min\limits_{\boldsymbol{\rho}} & g & \\ s.t. & f_1^{(k+1)}, f_2^{(k+1)}, ..., f_n^{(k+1)} \leq f^U & \\ & f_{n+1}, ..., f_m \leq 0 & \\ & V \leq \eta \cdot V_0 & \\ & \rho_\ell \leq \rho_{i,j} \leq 1 & i = 1, ..., N; j = 1, ..., L \\ & \rho_{i,\boldsymbol{d}(j)} \leq \rho_{i,\boldsymbol{d}(j+1)} & i = 1, ..., N; j = 1, ..., L-1 \end{array} \tag{20}$$

where the superscript k denotes the outcome after the k^{th} iteration, the starting point of this approximation, and $k+1$ denotes the outcome of this step. The subscript i denotes the node and ranges from 1 to N, j denotes the layer and runs from 1 until L. The structural responses that were the objectives, are now constraints, and allowed to increase, depending on the amount of grey area and the Lagrangian multipliers of these structural responses:

$$f^U = \max(f_1^{(k)}, f_2^{(k)}, ..., f_n^{(k)}) + \epsilon \cdot \frac{g}{\sum_{l=1}^{n} \lambda_l} \tag{21}$$

This relaxation has been proven to work well in previous work.[15]

B. Fibre angle optimisation

Seen as a function of the fibre angles, the first level approximation (18) no longer has a simple mathematical form and is not generally convex. Hence, a second level approximation is made based on the first level approximation in terms of the fibre angles:

$$f^{(2)} \approx f_0^{(1)} + \boldsymbol{g} \cdot \Delta\boldsymbol{\theta} + \Delta\boldsymbol{\theta}^T \cdot \boldsymbol{H} \cdot \Delta\boldsymbol{\theta} \tag{22}$$

where $f_0^{(1)}$ denotes the value, $\boldsymbol{g}$ the gradient and $\boldsymbol{H}$ the Gauss-Newton part of the Hessian of the first level approximation at the approximation point.[22] While optimising this second level approximation, a steering constraint is also taken into account to make sure the found laminate is manufacturable. The steering is defined as

$$\varsigma^2 = \frac{2}{\Omega} \cdot \boldsymbol{\theta}^T \cdot \boldsymbol{L} \cdot \boldsymbol{\theta} \tag{23}$$

where $\boldsymbol{L}$ is the standard FEM discretisation of the Laplacian. If this is taken to be the Laplacian of the complete layer, a global steering constraint is imposed, if the element Laplacian is used, a local steering constraint is imposed. The global steering constraint limits the number of gaps and overlaps, while the local steering makes sure the radius of curvature is not too small for the machine to lay down the fibre without wrinkling. The bound on steering value ς^U is the inverse of the minimal steering radius needed; for example: a maximal steering value of $2m^{-1}$, corresponds to a minimal steering radius of $500mm$. The optimisation problem can be written as

$$\begin{array}{lll} \min\limits_{\boldsymbol{\theta}} & \max(f_1, f_2, ..., f_n) & \\ s.t. & f_{n+1}, ..., f_m \leq 0 & i = 1, ..., N \\ & \varsigma_e \leq \varsigma^U & ; e = 1, ..., E \\ & \frac{-\pi}{2} \leq \theta_{ij} \leq \frac{\pi}{2} & i = 1, ..., N; j = 1, ..., L \end{array} \tag{24}$$

where E denotes the number of elements.

The details on the fibre angle optimisation, including the steering constraints, can be found in Peeters et al.[22]

IV. Solution Procedure

The two optimisation problems defined in the previous section, one for fibre angle optimisation and one for ply drop optimisation, are both solved in each iteration. After both are solved, a decision is made as

to which variable is updated and the current iterate is updated. In this section, first the solution of each sub-problem is discussed, then it is explained how both optimisations are combined. Before the optimisation of the sub-problem is started, the constraints are defined: local and global steering maxima are posed for the fibre angle optimisation, the dropping order is fixed for the ply drop optimisation.

A. Solution of the sub-problem

The approximations used for both fibre angle and ply drop optimisation are guaranteed to be convex. To ensure convergence to a (local) optimum, every step needs to be an improvement (i.e., reduced objective and feasible constraints). One possibility to guarantee this is to make each approximation conservative, meaning it is strictly greater than the function it approximates at the new iterate. To achieve this, Svanberg proposed to add a positive function to the approximations, referred to as damping function in the remainder which has zero function and gradient at the approximation point.[27] This damping function is scaled with a damping factor which is adjusted to make the approximations conservative. The damping factor is updated after each iteration: it is reduced if the new iterate is conservative with respect to the function it approximates, otherwise it is increased. The damping function for the second level approximation of the ply drop optimisation is given by

$$d^{(2)} = \sum_i \left(\frac{x_i}{x_{0i}} + \frac{x_{0i}}{x_i} - 2 \right) \cdot w_i \tag{25}$$

where w_i is defined as

$$w_i = \frac{A_i}{\sum_i A_i} \tag{26}$$

where A_i is the area represented by node i. The details of the damping function and damping factor can be found in Peeters et al.[22]

The optimisation procedure for both fibre angle and ply drop optimisation is the same. Starting from the level one approximation, the damping is added and the level two approximation is built. This system is solved using the interior-point predictor-corrector scheme, the damping factor of level two is updated and it is checked whether the level one approximation is improving. If it is improving, the level two approximations are updated, if not, the system is solved again with the updated damping factor. This is repeated until the level one approximation has converged or a maximum number of iterations is reached. The solution of the approximate sub-problem is performed using a predictor-corrector interior-point optimisation scheme.[28] A schematic overview of this code can be seen in Figure 2.

B. Combined ply drop and fibre angle optimisation

In this section, combining the two optimisation procedures, described in the previous section, is considered. A version of the coordinate descent method is used: after performing the optimisation with respect to both sets of variables (densities and angles), it is decided based on a criterion which set of variables is more useful to be updated. However, to make sure the optimisation is not dominated by either the densities or the angles, a maximum of three consecutive updates of the same variable is allowed.

In the first step of the optimisation, where the problems are described in equations (24) and (19), the decision criterion is clear: the variable that leads to the largest improvement in objective is updated. For the second step of the optimisation, where the problems are described in equations (24) and (20) , the criterion is not straightforward since both optimisations have a different objective and the criterion should be independent of the number of objectives and constraints. It was decided to update the variable which had the largest improvement in their respective objective function, but for the ply drop optimisation the possible improvement in structural performance was also taken into account. The improvement is thus defined according to

$$\begin{aligned} i_\rho &= g^{(k)} - g^{(k+1)} + \max\left({f_i}^{(k)}\right) + \epsilon \cdot \frac{g^{(k)}}{\sum_{j=1}^{n} \lambda_j} - \max\left({f_i}^{(k+1)}\right) \\ i_\theta &= \max\left({f_i}^{(k)}\right) - \max\left({f_i}^{(k+1)}\right) \end{aligned} \tag{27}$$

The grey values are the exact values, while the new values for the structural responses are the level one approximations.

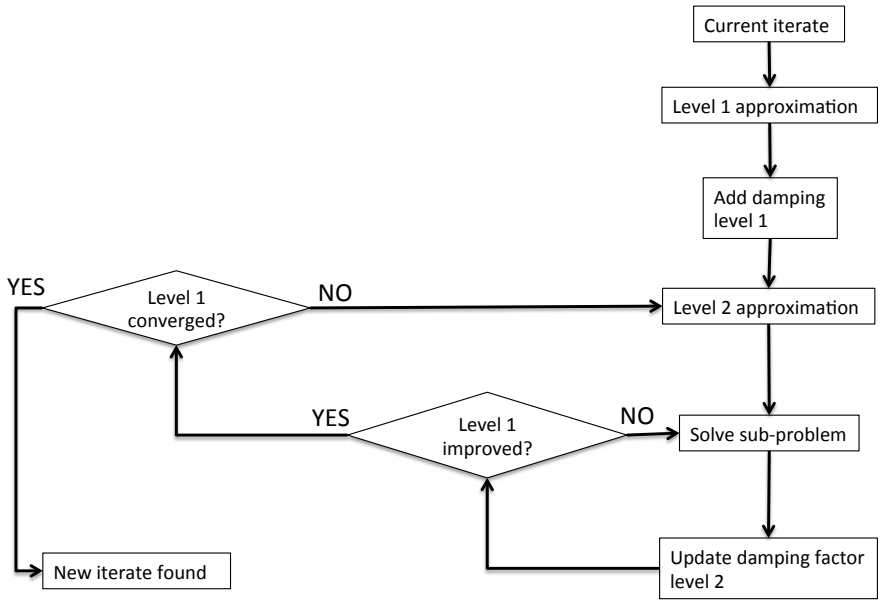

Figure 2. schematic overview of the code for a single optimisation step

Once it is determined which variable will be updated, the damping function of the level one approximation is updated and an FE analysis is performed to check whether the FE response improves. If this is not the case, the iterate is rejected and the optimisation for that variable is repeated. If the iterate is accepted, the variable is updated. The complete procedure is repeated until convergence, defined in this context as a change in objective function smaller than 10^{-3} between consecutive FE analyses normalised with respect to the quasi-isotropic response. A schematic overview of the code can be seen in Figure 3. The block 'optimise density distribution' was explained in section A. The block 'new iterate found' in Figure 2 is the output of the optimise density/fibre angle distribution shown in Figure 3.

V. Post-processing

The outcome of the optimisation is a fibre angle and fictitious density distribution, while a fibre placement machine needs fibre paths and exact ply boundaries: hence, two post-processing steps are done: one, the ply boundaries are determined for each ply, and two, the fibre paths are constructed.

To determine the ply boundaries, the density distribution is interpolated over the complete domain. Once this is done a certain threshold value, usually 0.7, is chosen and the contours are determined. These contours are then smoothed using the built-in Matlab function smooth to generate smooth contours for each ply. One consideration at this point is that to decrease chances of delaminations, a minimal distance between ply drops should be kept. This constraint is not implemented in the optimisation, the user should decide at this point whether or not to change certain boundaries to adhere to this minimal distance.

The determination of fibre paths from the fibre angle distribution is not discussed in this paper, the interested reader is referred to the paper by Blom.[29,30] Since the fibre angle distribution is defined over the complete structure, the fibre paths will also be found for the complete structure, and trimmed afterwards depending on the boundaries found in the previous step.

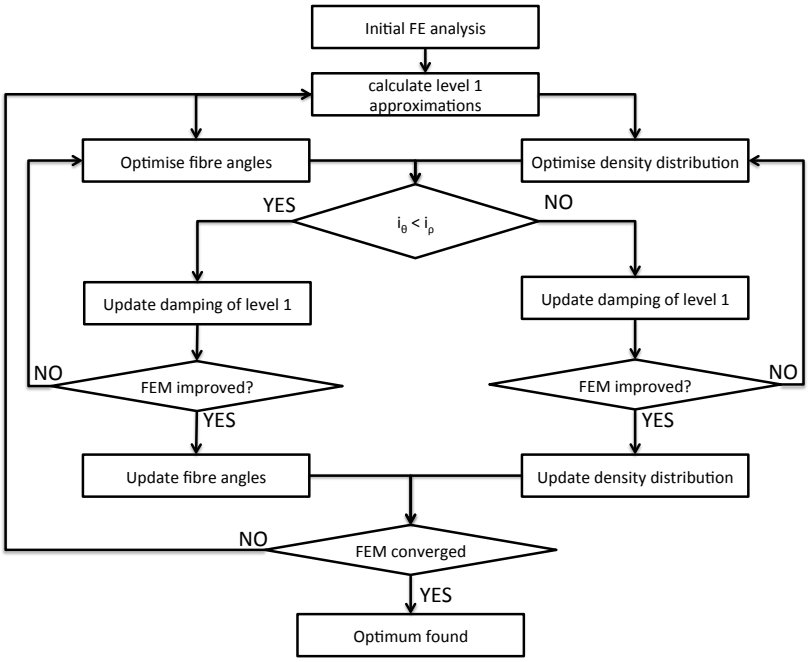

Figure 3. schematic overview of the code

VI. Results

The proposed formulation was tested for the buckling optimisation of a square plate with side length of 500 mm that is simply supported on two edges and subject to uni-axial compression load on the other two, as can be seen in Figure 4. The plate is meshed using 17 nodes on each side, leading to 289 nodes and 512 triangular elements . The material properties are given by: $E_1 = 177GPa$, $E_2 = 10.8GPa$, $G_{12} = 7.6GPa$ and $\nu_{12} = 0.27$. The maximum volume is the volume of a constant thickness laminate with 24 layers. A minimum of 8 layers and a maximum of 36 layers is posed. The objective is to minimise the maximum of the inverse of the first two buckling loads of the plate under the given load, subjected to the volume constraint. The first two buckling loads are used in the optimisation formulation to take mode jumping into account. For computational reasons, only a global steering constraint of $3m^{-1}$ (corresponding to a minimum average radius of curvature of $333mm$) is posed. Symmetry constraints around the x- and y-axes are imposed during the optimisation, reducing the number of variables by almost a factor of four, to 81 nodes. Furthermore, the laminate is assumed to be balanced and symmetric, with adjacent pairs of $\pm\theta$ layers. This means that each fibre angle or density actually represents four layers. The dropping order is defined as: $[7, 2, 8, 3, 6, 4, 5, 9, 1]$. There are 8 fixed layers: the outer layers (1) and layers around the symmetry plane (9) are always present. A graphical representation of the dropping order can be seen in Figure 5.

The results of the different optimisations are shown in Table 1. The optimisation used is indicated in the first column. If the laminate has a constant thickness laminate, this means it consists of 24 layers, hence all laminates have the same weight. The first two buckling loads normalised with respect to the critical buckling load of a quasi-isotropic laminate with the same weight are shown in the second and third column. The quasi-isotropic laminate is defined using lamination parameters: all in- and out-of-plane lamination parameters are set equal to zero, and the thickness of the laminate is constant, at 24 layers. The difference relative to a constant thickness, steered laminate optimised using the current optimiser is shown in the last column. The last row gives the converged solution after step 2, while the second to last row gives the result after step 1 of the optimisation.

Looking at the results in Table 1, it can be seen that allowing ply drops leads to large improvements in buckling load. One result that stands out is that the buckling load improves in the second step of the

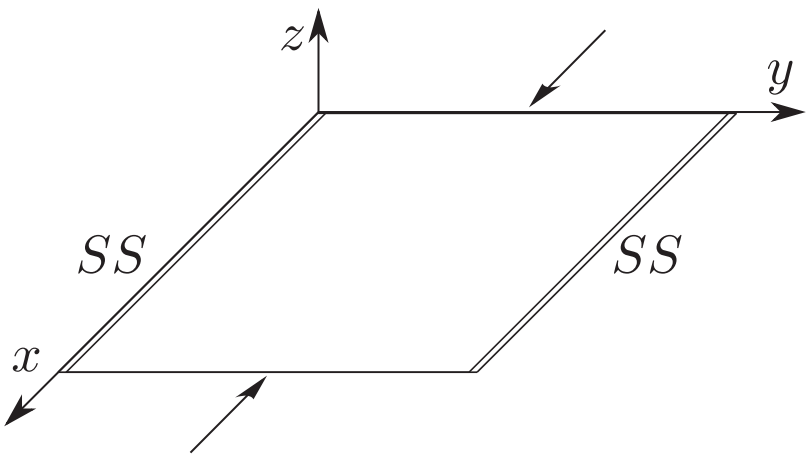

Figure 4. Load case and boundary conditions

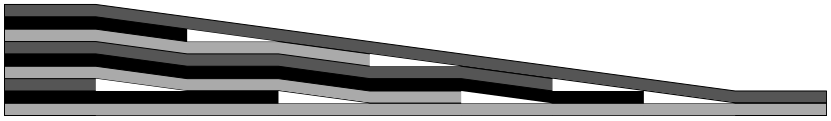

Figure 5. Visualisation of the dropping order

optimisation when both steering and ply drops are allowed. This is surprising at first, but it can be explained: the number of variables is increased in the second step and by dropping single plies, the difference in stiffness from one point to the next can be larger than when only the thickness of all plies is changed and the steering constraint is active. The result from the current optimiser is not as good as the final result from the stiffness optimisation, which is as expected since there are no steering constraints and the thickness is continuous in the stiffness optimisation.

Table 1. Overview of the results of the different optimisations

optimisation	buckling load 1	buckling load 2	difference w.r.t. constant thickness
steered fibres with constant thickness	2.620	2.645	0 %
lamination parameters with constant thickness	3.122	3.186	+ 19.2 %
lamination parameters with variable thickness	6.298	6.667	+ 140.4 %
straight fibres with ply drops	3.084	3.139	+ 17.7 %
steered fibres with variable thickness	4.301	4.316	+ 64.2 %
steered fibres with ply drops	4.868	4.869	+ 85.8%

When looking at the thickness distribution shown in Figure 6, it can be seen that the thickness distribution found using stiffness optimisation and the current optimiser is almost the same. Some small differences are observed, but the general lay-out is the same with the stiffener-like thickness build-up at the sides and the smaller enforcement in the middle. This also agrees well with the thickness distribution found by Joshi and Biggers.[13] As an example, two design layers and their balanced counterpart are shown in Figure 7: the layer at the outside, which completely covers the plate, is shown on the left. Almost no steering is observed, and the angles are almost $\pm 45°$, as one would expect for a buckling optimisation. On the right of Figure 7 layers 11 and 12 from the outside are shown. This is one of the layers that resembles a stiffener at the side, and at these places the angles go more towards $0°$ at the edges, and behave like a stiffener, which is again as expected.

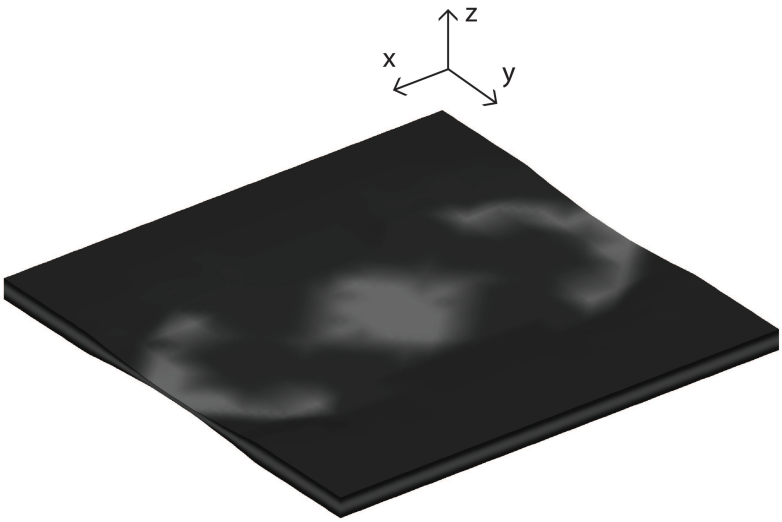

(a) thickness distribution found using current optimiser

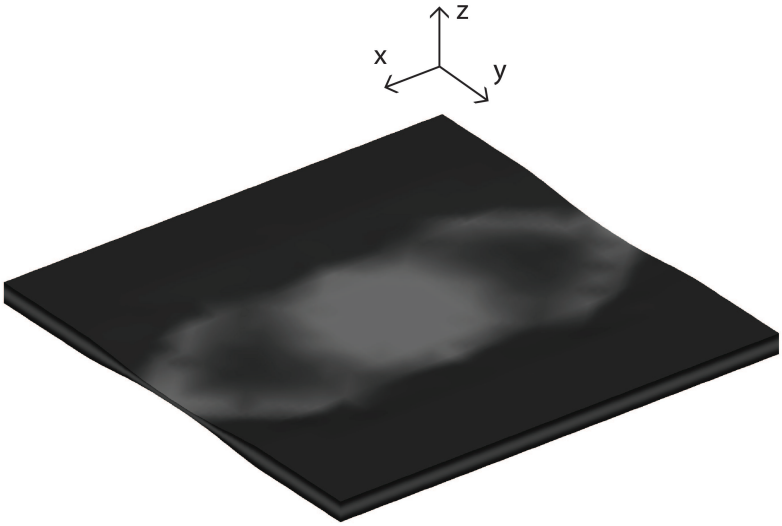

(b) Thickness distribution found using stiffness optimisation

Figure 6. Comparison of the thickness distribution found using stiffness optimisation and the current optimiser

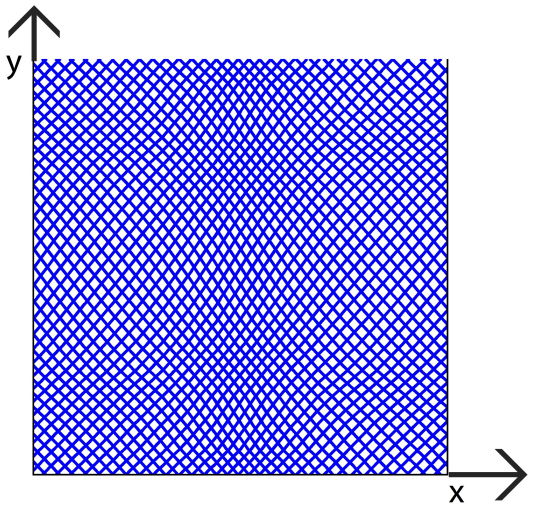

(a) Layer 1 and 2, at outside

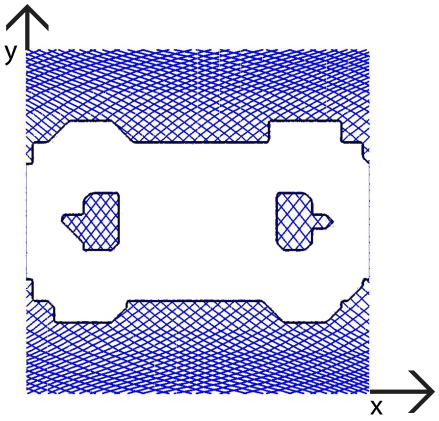

(b) Layer 11 and 12, starting from the outside (out of 18 until symmetry plane)

Figure 7. 4 layers from the complete 18 layer symmetric part of the laminate

As a second example, the same optimisation is repeated, but this time a stiffness constraint is added: the stiffness needs to be at least the stiffness of a quasi-isotropic, constant thickness laminate with the same weight. The results of the stiffness-constrained problem are shown in Table 2. It can be seen there is a large penalty, 22%, to the buckling load of a constant thickness laminate when stiffness is constrained. When only ply drops are used and no steering is allowed, the penalty is considerably smaller, 12.8 %. When both steering and ply drops are combined, the penalty, 13.2%, is of the same order as the case without steering. This may be explained by the increasing number of variables to optimise and the lack of constraints in the ply drop optimisation: the fibre angles have to satisfy the steering constraint which limits the change in mechanical properties from one point to the next, while there is no such constraint for the ply drop location optimisation. As in the unconstrained case, the optimal performance found using stiffness optimisation is better than that found using the combined fibre angle and ply drop optimisation. This is expected since stiffness optimisation should give an upper bound for performance. Furthermore, the buckling load is also almost the same (- 1 %) as that from the previous example which can be explained by the lack of manufacturing constraints.

Table 2. Overview of the results of the different optimisations

optimisation	buckling load 1	buckling load 2	stiffness	difference w.r.t. constant thickness
steered fibres with constant thickness	2.042	2.473	1.000	0 %
lamination parameters with constant thickness	2.109	3.151	1.000	+ 3.3 %
lamination parameters with variable thickness	6.236	6.344	1.000	+205.4 %
straight fibres with ply drops	2.688	2.692	1.002	+ 31.6 %
steered fibres with variable thickness	3.798	3.799	1.011	+ 86.5 %
steered fibres with ply drops	4.229	4.233	1.000	+ 107.1 %

Two design layers are shown in Figure 8 for the constrained optimisation. The two layers at the outside are shown on the left and again, the fibres are almost straight, and equal almost $\pm 45°$. The layers 11 and 12 from the outside are shown on the right and these again go towards $0°$on the right. Furthermore, a part in the middle appears to satisfy the stiffness constraint. The angle, however, is almost $\pm 45°$showing that the topology of this layer is stiffness-driven, but the angle buckling-driven.

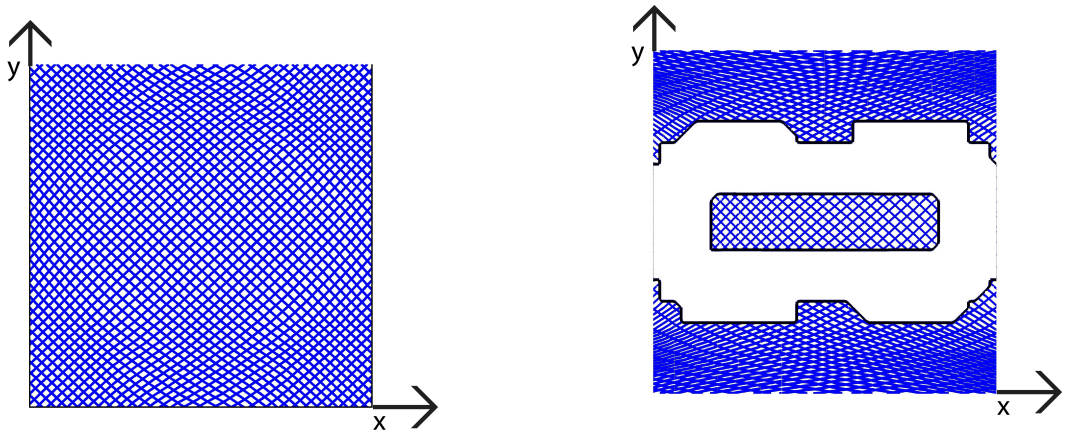

(a) Layer 1 and 2, at outside

(b) Layer 11 and 12, starting from the outside (out of 18 until symmetry plane)

Figure 8. 4 layers from the complete 18 layer symmetric part of the laminate

VII. Conclusion

In this paper, fibre angle and ply drop optimisation were combined to obtain steered, variable thickness composite laminates. Convex approximations were constructed of structural responses in terms of the fibre angle distribution or the fictitious density distribution. The method of successive approximations was used alternating between fibre-angle and density optimisation. The fictitious density distribution was optimised using a topology-like approach. The method of explicit penalisation was used to drive the fictitious densities to either zero or one. The optimisation was performed in two steps: in the first step the structural performance was optimised using total thickness and fibre angles as design variables, and in the second step the ply-by-ply density distribution was driven to either zero or one to obtain the optimal ply drop locations.

Initial results indicated the method performs well, and demonstrated the large performance improvements that can be reached by incorporating ply drops in the optimisation. A square, simply supported panel under uni-axial compression was optimised for buckling with and without a constraint on minimum axial stiffness. When the stiffness constraint is excluded the results showed that the buckling load could be improved, relative to the best steered constant thickness panel, by only using ply drops and no steering. The results also indicated that an even larger improvement may be attained by combining steering and ply drops. When the stiffness constraint was considered, the buckling load slightly decreased for the optimal steered, variable thickness laminate, while when only steering was used there was a significant decrease in buckling load. The results suggest that ply drops are an effective way to improve the buckling performance, with or without stiffness constraint, and that the proposed optimisation algorithm is able successfully to generate improved designs. Since ply drops change the material properties from one point to the next, much like steering does, it is expected also for stiffness and strength optimisation ply drops are an effective way to generate improved designs.

The current algorithm is limited in two respects: it cannot optimise the ply dropping sequence; this is pre-defined by the user, and it cannot maintain a minimum distance between consecutive ply drops. While extending the algorithm to address these issues can be the subject of future research, for practical applications, the ply drop boundaries and drop schedule may be adjusted by the designer to obtain manufacturable laminates using the current algorithm.

VIII. Acknowledgements

This work is supported by the CANAL (CreAting Non-conventionAl Laminates) Project, part of the European Union Seventh Framework Program.

References

[1]IJsselmuiden, S. T., *Optimal design of variable stffness composite structures using lamination parameters*, Ph.D. thesis, Delft University of Technology, 2011.

[2]Ijsselmuiden, S. T., Abdalla, M. M., and Gürdal, Z., "Optimization of Variable-Stiffness Panels for Maximum Buckling Load Using Lamination Parameters," *AIAA Journal*, Vol. 48, No. 1, 2010, pp. 134–143.

[3]Jung-Seok Kim, C.-G. K. and Hong, C.-S., "Optimum design of composite structures with ply drop using genetic algorithm and expert system shell," *Composite Structures*, Vol. 46, No. 2, 1999, pp. 171 – 187.

[4]Adams, D. B., Watson, L. T., Gürdal, Z., and Anderson-Cook, C. M., "Genetic algorithm optimization and blending of composite laminates by locally reducing laminate thickness," *Advances in Engineering Software*, Vol. 35, No. 1, 2004, pp. 35 – 43.

[5]IJsselmuiden, S. T., Abdalla, M. M., Seresta, O., and Gürdal, Z., "Multi-step blended stacking sequence design of panel assemblies with buckling constraints," *Composites Part B: Engineering*, Vol. 40, No. 4, 2009, pp. 329 – 336.

[6]Sørensen, S. and Stolpe, M., "Global blending optimization of laminated composites with discrete material candidate selection and thickness variation," *Structural and Multidisciplinary Optimization*, 2015, pp. 1–19.

[7]Liu, D., Toroporov, V. V., Querin, O. M., and Barton, D. C., "Bilevel Optimization of Blended Composite Wing Panels," *Journal of Aircraft*, Vol. 48, No. 1, 2015/07/01 2011, pp. 107–118.

[8]De Leon, D., de Souza, C., Fonseca, J., and da Silva, R., "Aeroelastic tailoring using fiber orientation and topology optimization," *Structural and Multidisciplinary Optimization*, Vol. 46, No. 5, 2012, pp. 663–677.

[9]Delgado, G., *Optimization of composite structures: A shape and topology sensitivity analysis*, Theses, Ecole Polytechnique X, June 2014.

[10]Sørensen, S. N., Sørensen, R., and Lund, E., "DMTO a method for Discrete Material and Thickness Optimization of laminated composite structures," *Structural and Multidisciplinary Optimization*, Vol. 50, No. 1, 2014, pp. 25–47.

[11]Lund, E., "Buckling topology optimization of laminated multi-material composite shell structures," *Composite Structures*, Vol. 91, No. 2, 2009, pp. 158 – 167.

[12]Sørensen, R. and Lund, E., "Thickness filters for gradient based multi-material and thickness optimization of laminated composite structures," *Structural and Multidisciplinary Optimization*, 2015, pp. 1–24.

[13]Joshi, M. G. and Jr, S. B. B., "Thickness optimization for maximum buckling loads in composite laminated plates," *Composites Part B: Engineering*, Vol. 27, No. 2, 1996, pp. 105 – 114.

[14]Kassapoglou, C., *Design and analysis of composite structures*, John Wiley and Sons, Ltd, 2010.

[15]Peeters, D., van Baalen, D., and Abdalla, M., "Combining topology and lamination parameter optimisation," *Structural and Multidisciplinary Optimization*, 2015, pp. 1–16.

[16]Irisarri, F.-X., Lasseigne, A., Leroy, F.-H., and Riche, R. L., "Optimal design of laminated composite structures with ply drops using stacking sequence tables," *Composite Structures*, Vol. 107, No. 0, 2014, pp. 559 – 569.

[17]Bailie J.A., Ley R.P., P. A., "A summary and review of composite laminate design guidelines," Tech. Rep. NAS1-19347, Northrop Grumman-Military Aircraft Systems Division, 1997.

[18]Z., X. and J., P., "Structural Optimization of Composite Wing Based on Different Blending Models Using Genetic Algorithm," *Applied Mechanics and Materials*, Vol. 401-403, 2013, pp. 886–890.

[19]Seresta, O., Gürdal, Z., Adams, D. B., and Watson, L. T., "Optimal design of composite wing structures with blended laminates," *Composites Part B-engineering*, Vol. 38, 2007, pp. 469–480.

[20]Sigmund, O. and Petersson, J., "Numerical instabilities in topology optimization: A survey on procedures dealing with checkerboards, mesh-dependencies and local minima," *Structural optimization*, Vol. 16, No. 1, 1998, pp. 68–75.

[21]de Wit, A. and van Keulen, F., "Numerical Comparison of Multi-Level Optimization Techniques," *48th AIAA/ASME/ASCE/AHS/ASC Structures, Structural Dynamics, and Materials Conference*, American Institute of Aeronautics and Astronautics, 2014/11/11 2007.

[22]Peeters, D. M., Hesse, S., and Abdalla, M. M., "Stacking sequence optimisation of variable stiffness laminates with manufacturing constraints," *Composite Structures*, Vol. 125, No. 0, 2015, pp. 596 – 604.

[23]Haftka, R. and Gürdal, Z., *Elements of Structural Optimization*, Contributions to Phenomenology, Springer Netherlands, 1992.

[24]Kumar, V., Lee, S.-J., and German, M., "Finite element design sensitivity analysis and its integration with numerical optimization techniques for structural design," *Computers and Structures*, Vol. 32, No. 34, 1989, pp. 883 – 897.

[25]Fleury, C., "CONLIN: An efficient dual optimizer based on convex approximation concepts," *Structural optimization*, Vol. 1, No. 2, 1989, pp. 81–89.

[26]Foldager, J., Hansen, J., and Olhoff, N., "A general approach forcing convexity of ply angle optimization in composite laminates," *Structural optimization*, Vol. 16, No. 2-3, 1998, pp. 201–211.

[27]Svanberg, K., "a class of globally convergent optimization methods based on conservative convex separable approximations," *Siam J. optim*, Vol. 2, 2002, pp. 555–573.

[28]Zillober, C., "A Combined Convex ApproximationInterior Point Approach for Large Scale Nonlinear Programming," *Optimization and Engineering*, Vol. 2, No. 1, 2001, pp. 51–73.

[29]Blom, A. W., Tatting, B. F., Hol, J. M., and Gürdal, Z., "Fiber path definitions for elastically tailored conical shells," *Composites Part B: Engineering*, Vol. 40, No. 1, 2009, pp. 77 – 84.

[30]Blom, A. W., Abdalla, M. M., and Gürdal, Z., "Optimization of course locations in fiber-placed panels for general fiber angle distributions," *Composites Science and Technology*, Vol. 70, No. 4, 2010, pp. 564 – 570.